

Dynamics of zebrafish locomotion being independent of spatial size

Zhen Wang(王震), Jian Gao(高见), Yongshang Long(龙永尚), Huaping Lv(吕华平), and Qun Wang(王群)

Citation: Chin. Phys. B, 2025, 34 (**3**): 038702. DOI: 10.1088/1674-1056/ada54c
Journal homepage: http://cpb.iphy.ac.cn; http://iopscience.iop.org/cpb

What follows is a list of articles you may be interested in

Studying the co-evolution of information diffusion, vaccination behavior and disease transmission in multilayer networks with local and global effects

Liang'an Huo(霍良安) and Bingjie Wu(武兵杰)
Chin. Phys. B, 2024, 33 (**3**): 038702. DOI: 10.1088/1674-1056/ad0114

Impact of individual behavior adoption heterogeneity on epidemic transmission in multiplex networks

Liang'an Huo(霍良安) and Yue Yu(于跃)
Chin. Phys. B, 2023, 32 (**10**): 108703. DOI: 10.1088/1674-1056/acea65

Discontinuous and continuous transitions of collective behaviors in living systems

Xu Li(李旭), Tingting Xue(薛婷婷), Yu Sun(孙宇), Jingfang Fan(樊京芳), Hui Li(李辉), Maoxin Liu(刘卯鑫), Zhangang Han(韩战钢), Zengru Di(狄增如), and Xiaosong Chen(陈晓松)
Chin. Phys. B, 2021, 30 (**12**): 128703. DOI: 10.1088/1674-1056/ac3c3f

A primary model of decoherence in neuronal microtubules based on the interaction Hamiltonian between microtubules and plasmon in neurons

Zuoxian Xiang(向左鲜), Chuanxiang Tang(唐传祥), Lixin Yan(颜立新)
Chin. Phys. B, 2019, 28 (**4**): 048701. DOI: 10.1088/1674-1056/28/4/048701

Analytically determining frequency and amplitude of spontaneous alpha oscillation in Jansen's neural mass model using the describing function method

Yao Xu(徐瑶), Chun-Hui Zhang(张春会), Ernst Niebur, Jun-Song Wang(王俊松)
Chin. Phys. B, 2018, 27 (**4**): 048701. DOI: 10.1088/1674-1056/27/4/048701

Dynamics of zebrafish locomotion being independent of spatial size

Zhen Wang(王震)[1], Jian Gao(高见)[1,†], Yongshang Long(龙永尚)[1], Huaping Lv(吕华平)[2], and Qun Wang(王群)[2]

[1] *School of Mathematics and Physics, Anqing Normal University, Anqing* 246011, *China*
[2] *School of Physics and Electronic Engineering, Jiangsu Normal University, Xuzhou* 221116, *China*

(Received 22 October 2024; revised manuscript received 7 December 2024; accepted manuscript online 3 January 2025)

Zebrafish are increasingly being utilized as a laboratory animal species to study various biological processes, both normal and pathological. It is crucial to comprehend the dynamics of zebrafish locomotion and put forth realistic models since their locomotion characteristics are employed as feedback indicators in diverse experiments. In this study, we conducted experimental research on the locomotion of zebrafish across various spatial sizes, focusing on the analysis of motion step size and motion direction. The results indicated that the motion step exhibits long-range correlations, the motion direction shows unbiased randomness, and the data characteristics are not influenced by spatial size. The dynamic mechanisms are complicated dynamical processes rather than fractional Brownian or Lévy processes motion. Based on the experimental results, we proposed a model for describing the movement of zebrafish in a circular container. Our findings shed light on the locomotion characteristics of zebrafish, and have the potential to benefit both the biological outcomes of animal tests and the welfare of the subjects.

Keywords: zebrafish locomotion, individual behavior, zebrafish modelling, stochastic process

PACS: 87.10.–e, 87.15.A–, 05.70.Ln

DOI: 10.1088/1674-1056/ada54c **CSTR:** 32038.14.CPB.ada54c

1. Introduction

As a vertebrate model species, zebrafish has great potential in the research of genetics, neurophysiology, and biomedicine.[1–4] Compared with other laboratory animals, zebrafish is rapidly becoming a popular laboratory species due to its high reproductive rate, short metabolic time, highly social behavior, and high breeding density.[5–9] For instance, zebrafish have been utilized in neurobehavioral studies,[10] genetic and biological investigations of both acute and chronic drug effects, and addiction research,[11,12] as well as in the exploration of higher neural functions of the brain, such as memory and learning.[13] In addition, in order to generate high-throughput behavioral data,[14–16] a lot of effort is being put into combining computer-generated imagery and robotic models of the same species, other species, and predators.[17–22]

Understanding the dynamics of zebrafish locomotion and developing accurate models is essential, as their locomotion characteristics serve as feedback indicators in various experiments.[23–25] Also, the necessity of comprehending the influence of spatial size on the dynamics characteristics of zebrafish locomotion arises from the inherent variations in the spatial and environmental contexts of individual subjects. The capacity to simulate intricate behaviors can enhance experimental protocols and hypotheses by facilitating in silico experiments, which can predict potential experimental outcomes without the need for animal testing. Within the framework of the three Russell's principle (replacement, reduction, and refinement),[26] virtual experiments can be utilized to conduct a priori power analysis to determine the required number of subjects, optimize the biological yield of experimental observations, and mitigate the impact of biological confounders. All these factors can contribute to reducing animal use and suffering. Additionally, models depicting the motion of individual fish serve as a crucial foundation for the modeling and analysis of collective fish behavior.[27–29]

Various models of individual animal locomotion have integrated uncorrelated and unbiased random walks, where the increments to an animal's position are assumed to be independent.[30,31] Recent studies have also investigated individual animal movement through the use of correlated random walks (CRWs).[28,32–35] In these studies, the assumption is that the animal's successive steps are correlated, as seen in the persistent random walker (PRW) model proposed in Ref. [32] for examining ant displacement and the CRW model proposed in Ref. [33] for investigating caribou movement. Recently, these processes have been adapted to characterize fish turn rate as a persistent turning walker (PTW).[35] Modeling the turn rate of the barred flagtail fish (Kuhlia mugil) as a stochastic mean-reverting process with a tendency towards zero captured its tendency to turn in both directions-left and right.[35]

Here, we conducted experimental research to investigate the locomotion characteristics of zebrafish. Subsequently, we developed a dynamic model to describe their movement, utilizing the experimental data. The following is the layout of this article. In Section 2, the methods are presented. The experimental results, which include motion trajectory, motion step

[†]Corresponding author. E-mail: gaojian1612@163.com

© 2025 Chinese Physical Society and IOP Publishing Ltd. All rights, including for text and data mining, AI training, and similar technologies, are reserved.

size and motion direction, are discussed in Section 3. The simulation results are outlined in Section 4. And the conclusion and discussion are given in Section 5.

2. Methods

2.1. Experiment

The test subjects employed zebrafish that were more energetic. Zebrafish were employed as the experimental model in our research. The subjects were between 6 and 8 months old, with an average body length of approximately 3 cm. The fish were housed in aquariums measuring 40 cm×24 cm×25 cm, with a maximum capacity of 25 fishes per tank. They were fed standard small fish food daily at 7 p.m. The experiment commenced following a 10-day acclimation period. The experimental apparatus comprised basins with radii of 9.5 cm (space *S*), 11.5 cm (space *M*), and 16.5 cm (space *L*). The water was consistently kept at a depth of 10 cm. The water temperature was maintained at 25 ± 1 °C, and the pH was kept at 7.0. To observe the fish, a high-resolution wide-angle camera (SONY FDR-AX60) was installed 100 cm above the water surface. All experiments were conducted under natural light during the daytime. For each experiment, a singular fish was placed in the basin, enabling it to move freely. The duration of each experiment was approximately 10 minutes. Before each experiment, we randomly selected an individual from the water tank, allowed it to acclimatize in the round experimental container for 30 minutes, and then commenced the experiment. Additionally, the water in the container was changed each time to prevent any influence from the previous fish on the experimental conditions. Conduct 10 experiments in each container, using different individuals for each experiment. The experiments in containers *S*, *M*, and *L* are denoted as groups *S*, *M*, and *L*, respectively. The individuals in the experiments can be referred to as group–individual, with (group = *S*, *M*, *L*) and (individual = 1, 2, 3, …, 10). We randomly selected one experiment from each of the three groups (*S*, *M*, and *L*) as examples and provided detailed descriptions in the text. The corresponding individuals are denoted as *S*–*s*, *M*–*s*, and *L*–*s*, respectively, and this group of 3 individuals is called group *s*.

2.2. Data

Our high-definition camera captures the experiments at 30 Hz, and the obtained videos were then processed using the open-source software Tracker (Version 6.2.0), thus allowing us to obtain the movement data of the zebrafish in each experiment. By processing these data, we can get the swimming track, step length, and movement direction of the zebrafish. The movement step of the fish at time t, which is the displacement within 0.1 s, can be expressed as movestep length$(t) = |\Delta \boldsymbol{X}(t)| = |\boldsymbol{X}(n+3) - \boldsymbol{X}(n)|$. $\boldsymbol{X}$ represents the displacement of a single fish, t is (n/30 s), and n ($n = 3, 6, 9, \ldots$) is the number of frames of the video. We use the angle between $\Delta \boldsymbol{X}(t)$ and the x-axis to represent the direction of motion $\theta(t)$. Similarly, we can calculate the change in direction of motion, $\Delta\theta(t)$, by $\Delta\theta(t) = \theta(t+0.1s) - \theta(t)$, which has a range of $[-\pi, \pi]$.

2.3. Model

Based on the analytical results of experimental data, we formulated a model that elucidates the movement of zebrafish in a circular basin with a radius of r. The equation of the model can be expressed as Eq. (1), where the vector $\boldsymbol{Q}_n$ denotes the location of the zebrafish with the basin's center as its origin. The sequence $\{M_1, M_2, M_3, \ldots\}$ and $\{\boldsymbol{d}_1, \boldsymbol{d}_2, \boldsymbol{d}_3, \ldots\}$ denote the time series of movement steps and directions, respectively. And the dynamic mechanism of $\{M_1, M_2, M_3, \ldots\}$ is fractional Brownian motion (fBm) which can be either derived from experimental data or generated manually. To accurately simulate the motion of zebrafish in a basin, the magnitude of the position vector should not be greater than the radius r. So, whenever an individual is about to cross the boundary, the individual can automatically select an appropriate direction to ensure that it does not cross the boundary. The rules for automatic direction selection are Eq. (2). The symbol Z indicates that the first $g_{n,i}$ is selected from the sequence G_n in order to prevent Q_{n+1} from exceeding r. Moreover, $g_{n,i}$ is calculated as shown in Eqs. (3) and (4)

$$\boldsymbol{Q}_{n+1} = \boldsymbol{Q}_n + M_n \boldsymbol{d}_{n+1}, \tag{1}$$

$$\boldsymbol{d}_{n+1} = Z\{g_{n,i};\quad i = 1,2,3,\ldots\} = ZG_n, \tag{2}$$

$$\boldsymbol{g}_{n,i} = \boldsymbol{h}_{n,i},\quad Q_n < r - r_r, \tag{3}$$

$$\boldsymbol{g}_{n,i} = \boldsymbol{h}_{n,i} + \boldsymbol{\chi}_{n,i},\quad r - r_r < Q_n < r,$$
$$n = 1,2,3,\ldots, \tag{4}$$

with

$$\begin{aligned}
\boldsymbol{\chi}_{n,i} &= \boldsymbol{e}'_{n,i} + \boldsymbol{e}''_{n,i},\\
\boldsymbol{e}'_{n,i} &= \frac{\alpha}{\rho},\\
\boldsymbol{e}''_{n,i} &= \beta\rho,\\
H_n &\equiv \{\boldsymbol{h}_{n,i};\quad i = 1,2,3,\ldots\}\\
&= \varphi\left(\boldsymbol{d}_n, \{\zeta\cdot\theta_{n,i};\quad i = 1,2,3,\ldots\}\right)\\
&= \varphi\left(\boldsymbol{d}_n, (\zeta\cdot\Theta_n)\right),
\end{aligned} \tag{5}$$

where $\boldsymbol{\chi}_{n,i}$ represents the boundary effect, and $\boldsymbol{\chi}_{n,i}$ can be decomposed into boundary tangential action $\boldsymbol{e}'_{n,i}$ and boundary normal phase action $\boldsymbol{e}''_{n,i}$. $\rho \equiv 1/r^2$, r_{r} is the distance at which the boundary effects. φ means to rotate the vector $\boldsymbol{d}_{n,i}$ at an angle $\theta_{n,i}$. The movement of zebrafish can be regarded as consisting of a large number of gliding processes, in which the direction of motion remains unchanged. When two gliding processes intersect, the direction change is a random process, which can be controlled by noise. The duration t_{f} of each gliding process is also a random process, and t_{f} follows a uniform

distribution in the interval $(0, \tau)$. The value of parameter ζ is 0 or 1 to control whether noise affects the motion discovery of zebrafish. $\Theta_n = \psi(W)$ is noise, and W is noise that follows the Weibull distribution of parameters a and b. The purpose of the symbol ψ is to randomly multiply the noise W by -1 or 1.

To facilitate comparison with our experimental results, we fixed all other parameters while only r was used as the control parameter, and the fixed values of other parameters were $\alpha = 0.01$, $\beta = 2.57$, $r_\tau = 0.3$, $\tau = 16$. Through experimentation, it was determined that the values of a and b are 0.29 and 0.76 respectively (see Fig. 7(d)).

2.4. Weibull distribution

By observing the distribution of movement steps and movement direction, it is found that their distribution has the characteristics of asymmetric distribution, and the Weibull distribution can flexibly depict this trend through its shape parameters and scale parameters. Therefore, in this paper, we use the Weibull distribution to fit the distribution of movement steps and movement direction.

The probability density function of the Weibull distribution is

$$f(y|a,b) = \frac{a}{b}\left(\frac{y}{a}\right)^{b-1} \exp\left[-\left(\frac{y}{a}\right)^{b}\right], \quad y \geq 0,$$
$$f(y|a,b) = 0, \quad y \leq 0. \tag{6}$$

The cumulative distribution function of the Weibull distribution is

$$\begin{aligned} p &= F(y|a,b) \\ &= \int_0^y \frac{b}{a}\left(\frac{y'}{a}\right)^{b-1} \exp\left[-\left(\frac{y'}{a}\right)^{b}\right] \mathrm{d}y' \\ &= 1 - \exp\left[-\left(\frac{y}{a}\right)^{b}\right]. \end{aligned} \tag{7}$$

The probability p that a single observation from the Weibull distribution with parameters a and b is within the interval $[0, y]$ can be obtained.

3. Experimental results

In our experiments, we investigated the movement characteristics of zebrafish. To capture general patterns, we utilized three containers of varying sizes (see Section 2 for details).

3.1. Movement trajectory

Movement trajectories are the basis for further analysis and can also reflect the individuals' movement characteristics at a macro level (see Fig. 1). Each individual's movement trajectory in space S covers the entire space, as depicted in Fig. 1(a) showing the movement trajectory of the individual S–s. The trajectories of other individuals in group S are depicted in Fig. S1 (Figures S1–S30 are shown in the supplementary materials). The distribution of trajectories in space S are relatively dense. The trajectories in space M are mostly distributed near the boundary [see Figs. 1(b) and S2], and the trajectories in space L are almost distributed along the boundary [see Figs. 1(c) and S3].

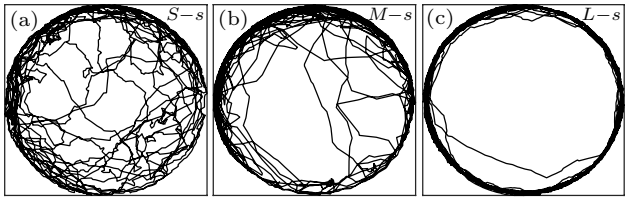


Fig. 1. Movement trajectories of the three individuals in group s. Trajectories in panels (a), (b), and (c) are those of zebrafish in basins with radii of 9.5 cm, 11.5 cm, and 16.5 cm, respectively.

We also calculated the distribution probability of distance of the individual from the center of the container for the three individuals in Fig. 1, as shown in Fig. 2. We find that individuals in different spaces occupy a larger proportion of the distribution at the boundary of the container. As the space size increases, the distribution near the center of the container significantly decreases. These results indicate that the distribution characteristics of trajectories in containers of different sizes are completely different. The difference in these distributions can reflect the attractiveness of the boundary to individuals, and this attractiveness decreases as the curvature of the boundary increases. These trajectories are composed of a series of line segments of varying lengths, indicating that the movement of zebrafish is composed of a large number of gliding movements. These features provide a basis for modeling the movement of zebrafish.

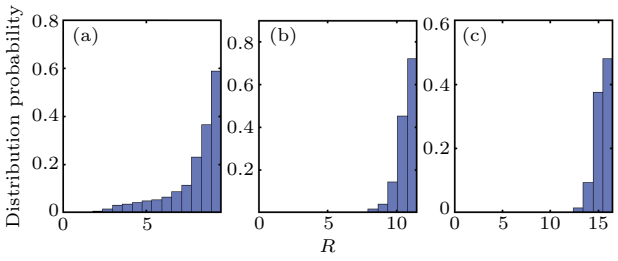


Fig. 2. The distribution probability of R for the three individuals in Fig. 1. R denotes the distance of the individual from the center of the container.

3.2. Movement step length

We obtained the time series data for the step lengths (measured as displacement per 0.1 second) of individuals' movements. The time series of step lengths for the three individuals in group s are depicted in Fig. 3(a) (corresponding to the trajectories in Fig. 1). And the frequency distribution of the step lengths of the three individuals are shown in Fig. 3(b). The cumulative frequency distributions of the corresponding step lengths are shown in Fig. 3(c). For other individuals in groups

S, *M*, and *L*, step lengths' frequency distributions and cumulative frequency distributions are shown in Figs. S4–S9. The results indicate that the step lengths series of zebrafish follows the Weibull distribution.

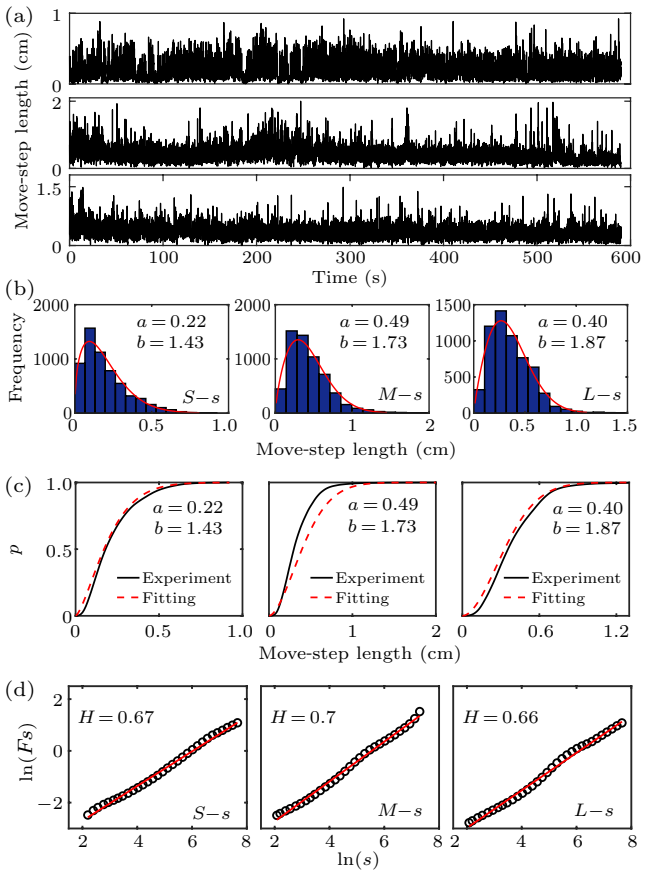


Fig. 3. Analysis results of the movement steps in Fig. 1. (a) The time series of the movement steps of the three individuals in Fig. 1. (b) Frequency distributions of movement steps in panel (a). The Weibull distribution was fitted to the data, resulting in the red curve. Both parameters a and b represent the parameters of the fitted curve. (c) Cumulative frequency distributions. The fitting curves are Weibull cumulative distribution. (d) The relationship between $\ln(s)$ and $\ln(Fs)$ of the time series in panel (a). The solid red lines are fitting curves, and the slope of fit curves are referred to as the Hurst index, denoted as H.

Figure 3(d) shows the $\ln(Fs)$ as a function of $\ln(s)$ for the step lengths series of the individuals in group *s*. Here, we use the detrended fluctuation analysis (DFA)[36,37] method for analysis. The value $\ln(s)$ represents the logarithm value of the time scale *s*, where *s* is the length of the window, representing the analysis of the sequence at different scales. Fs is the wave function of the time series calculated in the window corresponding to the step size *s*, which represents the detrended fluctuation amplitude of the series under different scales. The relationships of $\ln(Fs)$ and $\ln(s)$ for other zebrafish are depicted in Figs. S10–S12. Along a wide scale range, the data points for the series are closely distributed along the fitting lines, where the slope of the fitting line represents the Hurst index, denoted as H. These results ($H > 0.5$) indicate that the step lengths of individuals in all three containers exhibit long-range correlation.

We also considered the correlation-dependent balance estimation of diffusion entropy (cBEDE) method[38–40] to examine the scale-invariance. The relationships between S_{cBEDE} and $\ln(s)$ for the individuals in group *s* are illustrated in Fig. 4. Here, S_{cBEDE} is the diffusion entropy derived from each dataset using the cBEDE method. It serves as a quantitative measure to assess the scale-invariant behavior of time series data by estimating the entropy associated with the temporal dynamics across different time windows. This value not only reflects the intrinsic complexity of the dataset but also captures how the distribution of temporal patterns evolves with the size of the time window *s*. The curves of other individuals can be seen in Figs. S13–S15. The data points are closely packed along their respective fitting lines across a broad range, and the curves observed to a great extent follow the power law. The slopes of the fitting lines represent the scaling exponent, denoted as α.

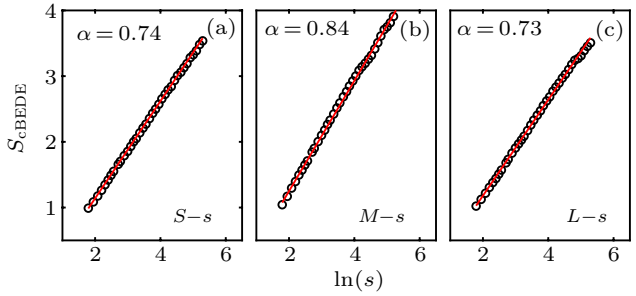


Fig. 4. The curves of S_{cBEDE} versus $\ln(s)$ of three individuals in group *s*. Panels (a), (b), and (c) are the results corresponding to individuals in *S*–*s*, *M*–*s*, and *L*–*s*, respectively. The slopes of fitting curves are the scaling exponent, denoted as α.

To examine whether the size of the activity space has an impact on the Hurst index and scaling exponent of the step lengths, we compared the average values of all experimental results in different containers (see Fig. 5). The results indicate that the average values of Hurst index H for all containers are around 0.66, and the average values of scaling exponent α are around 0.80. It can be seen that although the characteristics of trajectories in different containers show significant differences, there is no significant difference in the Hurst index H and scaling exponent α.

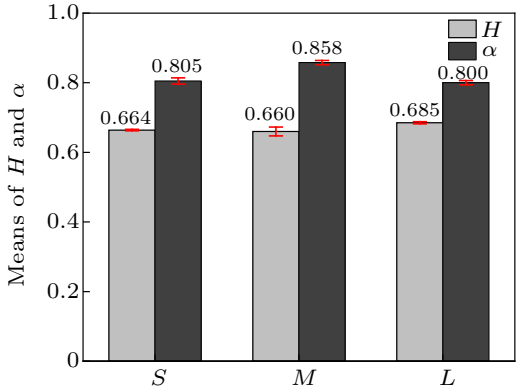


Fig. 5. The mean values corresponding to the Hurst index and scaling exponent in spaces *S*, *M*, and *L*.

The combined utilization of the scaling exponent α, as estimated by the cBEDE, and the Hurst index H, as estimated by the DFA, may illuminate the dynamical mechanisms underlying the series of step lengths of zebrafish. Specifically, the dynamical mechanism is fBm when H and α satisfy the relationship $\alpha = H$, and the dynamical mechanism is Lévy walk when H and α satisfy $\alpha = 1/(3-2H)$.[41] The relationships between α and H corresponding to the groups S, M, and L are shown in Fig. 6. For comparisons, we presented the curves $\alpha = H$ (black solid line) and $\alpha = 1/(3-2H)$ (red dotted line). The data points (H, α) of all individuals in the spaces S, M, and L are basically not distributed on the curves $\alpha = H$ and $\alpha = 1/(3-2H)$. Therefore, the individuals' step lengths in the spaces S, M, and L are generated by complex dynamical processes rather than Lévy processes or fBm.

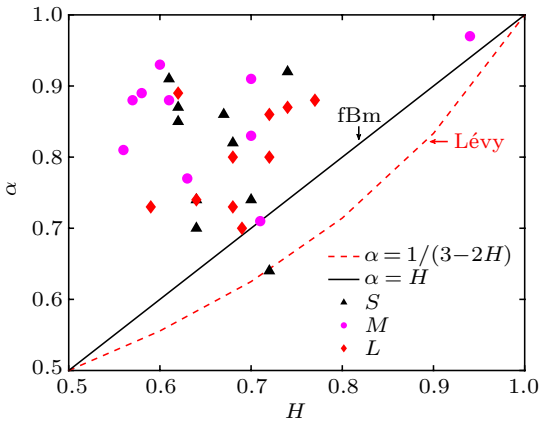


Fig. 6. The relationship between the scaling exponent α and the Hurst index H, which are obtained by the cBEDE and DFA methods, respectively. Solid black line and dashed red line represent $\alpha = H$ and $\alpha = 1/(3-2H)$, respectively.

3.3. Movement direction

The movement of zebrafish can be decomposed into step length and direction. Here, we analyzed the changes in movement direction $\Delta\theta$ for individuals. As depicted in Fig. 7, the experimental results of $\Delta\theta$ for the individuals in group s are presented. The experimental results of other individuals are shown in Figs. S16–S24. Figure 7(a) shows the time series of $\Delta\theta$ for the individuals in group s. The Hurst indexes and scaling exponents are both around 0.5, indicating that the change in direction is a general random process [see Figs. 7(b) and 7(c)]. Since the time series of $\Delta\theta$ is a general random process, and its frequency distribution is basically symmetric with respect to $\Delta\theta = 0$, so a more convenient way to study the change of direction is to consider $|\Delta\theta|$. The frequency distribution and cumulative frequency distribution of $|\Delta\theta|$ is shown in Figs. 7(d) and 7(e), respectively. The results show that the cumulative frequency distribution and frequency distribution of $|\Delta\theta|$ obey a Weibull cumulative distribution and a Weibull distribution, respectively, providing support for modeling the movement of zebrafish.

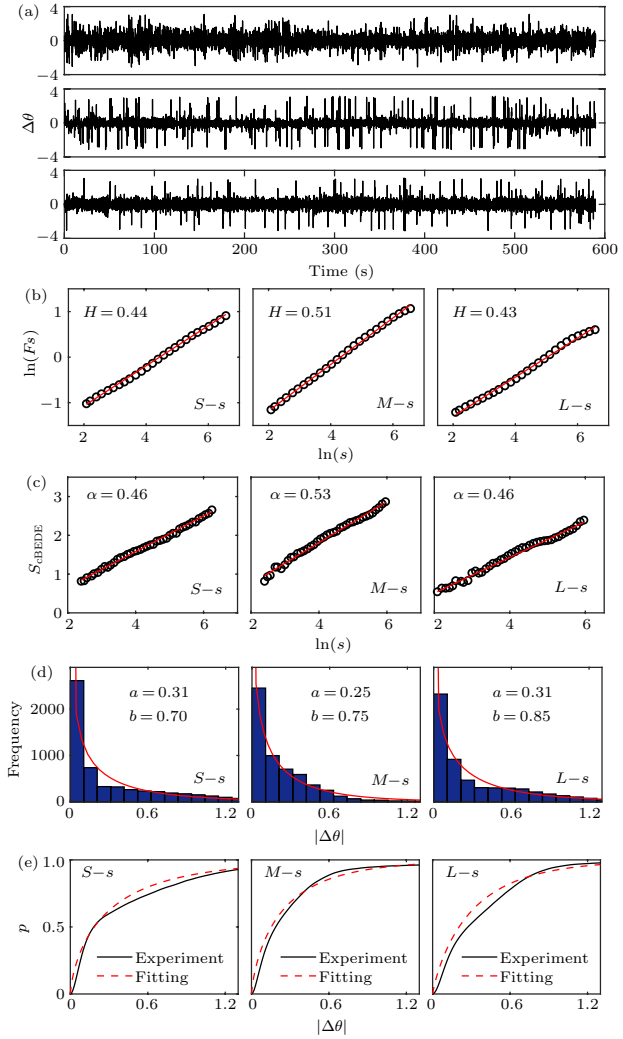


Fig. 7. Analysis results of changes in movement direction of the three individuals in group s. (a) Time series of changes in movement direction $\Delta\theta$. (b) The relationship between $\ln(Fs)$ and $\ln(s)$ of the time series of $\Delta\theta$. (c) Curves of S_{cBEDE} and $\ln(s)$. (d) Frequency distributions of $\Delta\theta$. The solid red curves are the corresponding fitting results of the Weibull distribution. (e) Cumulative frequency distributions of $\Delta\theta$. The solid red curves are the corresponding fitting results of the Weibull cumulative distribution.

4. Simulation results

Based on the experimental data, we developed a mathematical model to depict the movement of zebrafish within a circular container. In comparison with the experimental results, we selected the radius r of the circular container as the control parameter and examined its impact on the trajectories of zebrafish. The simulation duration matches the experimental duration, which is 10 minutes. Figure 8 illustrates the simulation results obtained using various values of r. The trajectory is evenly distributed in space when the radius r is equal to 9.5 cm [see Fig. 8(a)]. With a radius r of 11.5 cm, the trajectories predominantly adhere to the inner wall of the container, resulting in a substantial decrease in trajectory within the container [see Fig. 8(b)]. When the radius r equals 16.5 cm, nearly

all trajectories adhere to the inner wall of the container. The Hurst index H and scale index α of the step sequence from the simulation results under different radii were also calculated [Fig. 8(b)]. The results indicate that the step of the simulation at different radii is still generated by a complex process, rather than Lévy processes or fBm. This aligns with the experimental results, further validating the effectiveness of our model in describing zebrafish movement.

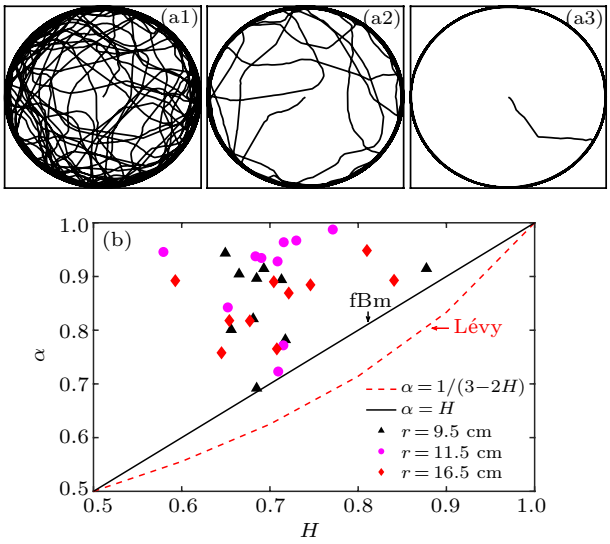


Fig. 8. (a) Simulation results of movement trajectories with different r: (a1) $r = 9.5$ cm, (a2) $r = 11.5$ cm, and (a3) $r = 16.5$ cm. (b) The relationship between the scaling exponent α and the Hurst index H of the step series of simulation results with different r.

5. Discussion and conclusion

Our experimental research analyzed the locomotion characteristics of zebrafish and then we established a dynamical model to describe the movement of zebrafish, utilizing the gathered experimental data. The results showed that the step lengths of zebrafish in a circular container displays long-range correlation. The change in direction of an individual during movement is a general stochastic process. The dynamic mechanisms are complex dynamical processes, distinct from fractional Brownian or Lévy processes motion, and the spatial size does not impact the dynamic mechanisms.

Human observation-based methods play a crucial role in behavioral studies of zebrafish, constituting an essential toolset for analysis.[14,15] Together with newly implemented tracking-based tools.[42,43] these methods have significantly advanced our comprehension of zebrafish behavior. These models can be utilized to conduct customizable exploratory in silico experiments before resorting to animal testing. Computational trials can enhance the biological yield of animal tests by optimizing the informational value of the trials. In addition, computational trials can contribute to subject welfare by enhancing the reliability of power analysis and reducing the influence of biological confounds.

Acknowledgements

Project supported by the National Natural Science Foundation of China (Grant No. 12205006) and the Excellent Youth Scientific Research Project of Anhui Province, China (Grant No. 2022AH030107).

References

[1] Vascotto S G, Beckham Y and Kelly G J 1997 *Biochem. Cell. Biol.* **75** 479
[2] Grunwald D J and Eisen J S 2002 *Nat. Rev. Genet.* **3** 717
[3] Rubinstein A L 2003 *PubMed* **6** 218
[4] Amsterdam A and Hopkins N 2006 *Trends Genet.* **22** 473
[5] Barbazuk W B 2000 *Genome Res.* **10** 1351
[6] Lieschke G J and Currie P D 2007 *Nat. Rev. Genet.* **8** 353
[7] Spence R, Gerlach G, Lawrence C and Smith C 2007 *Nat. Rev. Genet.* **83** 13
[8] Dooley K 2000 *Curr. Opin. Genet. Dev.* **10** 252
[9] Zhang N N, Zhou L Y, Liu X, Wei Z C, Liu H Y, Lan S, Meng Z and Fan H H 2020 *Chin. Phys. B* **30** 044204
[10] Stewart A, Gaikwad S, Kyzar E, Green J, Roth A and Kalueff A V 2012 *Neuropharmacology* **62** 135
[11] Gerlai R, Lahav M, Guo S and Rosenthal A 2000 *Pharmacol. Biochem. Behav.* **67** 773
[12] Mathur P and Guo S 2010 *Neurobiol. Dis.* **40** 66
[13] Al-Imari L and Gerlai R 2008 *Behav. Brain Res.* **189** 216
[14] Kalueff A V, Gebhardt M, Stewart A M, Cachat J M, Brimmer M, Chawla J S, Craddock C, Kyzar E J, Roth A, Landsman S, Gaikwad S, Robinson K, Baatrup E, Tierney K, Shamchuk A, Norton W, Miller N, Nicolson T, Braubach O and Gilman C 2013 *Zebrafish* **10** 70
[15] Maximino C, de Brito T M, da Silva Batista A W, Herculano A M, Morato S and Gouveia A 2010 *Behav. Brain Res.* **214** 157
[16] Kalueff A V, Stewart A M and Gerlai R 2014 *Trends Pharmacol. Sci.* **35** 63
[17] Saverino C and Gerlai R 2008 *Behav. Brain Res.* **191** 77
[18] Polverino G, Abaid N, Kopman V, Macri S and Porfiri M 2012 *Bioinspir. Biomim.* **7** 036019
[19] Luca R M and Gerlai R 2012 *Behav. Brain Res.* **226** 66
[20] Cianca V, Bartolini T, Porfiri M and Macri S 2013 *PLoS One* **8** e69661
[21] Abaid N, Bartolini T, Macri S and Porfiri M 2012 *Behav. Brain Res.* **233** 545
[22] Gokce S and Kayacan 2016 *Chin. Phys. B* **25** 010508
[23] Li F, Lin J, Liu X, Li W, Ding Y, Zhang Y and Li Q 2018 *Ann. Transl. Med.* **6** 173
[24] Giacomini N J, Rose B, Kobayashi K and Guo S 2006 *Neurotoxicol. teratol.* **28** 245
[25] Belyaeva N F, Kashirtseva V N, Medvedeva N V, Khudoklinova Yu Yu, Ipatova O M and Archakov A I 2009 *Biochem. Mosc. Suppl. S.* **3** 343
[26] Russell W M S and Burch R L 1960 *Med. J. Aust.* **1** 500
[27] Sumpter D 2010 *Collective Animal Behavior* (Princeton Univ. Press)
[28] Gautrais J, Ginelli F, Fournier R, Blanco S, Soria M, Chate H and Theraulaz G 2012 *PLoS Comput. Biol.* **8** e1002678
[29] Herbert-Read J E, Perna A, Mann R P, Schaerf T M, Sumpter D J T and Ward A J W 2011 *Proc. Natl. Acad. Sci. USA* **108** 18726-18731
[30] Codling E A, Plank M J and Benhamou S 2008 *J. R. Soc. Interface* **5** 813
[31] Giuggioli L, Potts J R and Harris S 2011 *Phys. Rev. E* **83** 061138
[32] Kareiva P and Nanako Shigesada 1983 *Oecologia* **56** 234
[33] Bergman C M, Schaefer J A and Luttich S N 2000 *Oecologia.* **123** 364
[34] Degond P and Motsch S 2008 *J. Sta. Phys.* **131** 989
[35] Gautrais J, Jost C, Soria M, Campo A, Motsch S, Fournier R, Blanco S and Theraulaz G 2008 *J. Math. Biol.* **58** 429
[36] Peng C K, Buldyrev S V, Havlin S, Simons M, Stanley H E and Goldberger A L 1994 *Phys. Rev. E* **49** 1685
[37] Tang Y F, Liu S L, Jiang R H and Liu Y H 2013 *Chin. Phys. B* **22** 030504
[38] Feng W, Yang Y, Yuan Q, Gu C and Yang H 2019 *Fractals* **27** 1950005
[39] Paolo Grigolini, Palatella L and Raffaelli G 2001 *Fractals* **09** 439
[40] Zhang W, Qiu L, Xiao Q, Yang H, Zhang Q and Wang J 2012 *Phys. Rev. E* **86** 056107
[41] Scafetta N and Grigolini P 2002 *Phys. Rev. E* **66** 036130
[42] Cachat J, Stewart A, Utterback E, Hart P, Gaikwad S, Wong K, Kyzar E, Wu N and Kalueff A V 2011 *PLoS One* **6** e17597
[43] Butail S, Bartolini T and Porfiri M 2013 *PLoS One* **8** e76123